

Void Shape Identification in a 2D Point Distribution

Netzer Moriya

1 Abstract

We introduce a new approach for identifying and characterizing voids within two-dimensional (2D) point distributions through the integration of Delaunay triangulation and Voronoi diagrams, combined with a Minimal Distance Scoring algorithm.

Our methodology initiates with the computational determination of the Convex Hull vertices within the point cloud, followed by a systematic selection of optimal line segments, strategically chosen for their likelihood of intersecting internal void regions. We then utilize Delaunay triangulation in conjunction with Voronoi diagrams to ascertain the initial points for the construction of the maximal internal curve envelope by adopting a pseudo-recursive approach for higher-order void identification. In each iteration, the existing collection of maximal internal curve envelope points serves as a basis for identifying additional candidate points. This iterative process is inherently self-converging, ensuring progressive refinement of the void's shape with each successive computation cycle. The mathematical robustness of this method allows for an efficient convergence to a stable solution, reflecting both the geometric intricacies and the topological characteristics of the voids within the point cloud.

We apply our method to two distinct point set ensembles: a canonical single circle with random dispersion along the circumference, and a pair of congruent circles with an intentionally created internal void. In both examined cases, the method effectively unveils the internal void shape, pinpointing key vertices that delineate its contours. Additionally, this approach allows for a degree of control over the intricacies of the internal shape, demonstrating its refining in capturing geometric details.

Our findings introduce a method that aims to balance geometric accuracy with computational practicality. The approach is designed to improve the understanding of void shapes within point clouds and suggests a potential framework for exploring more complex, multi-dimensional data analysis.

2 Introduction

Given a finite set $P = \{p_1, p_2, \dots, p_n\}$ where each point $p_i \in P$ is a tuple (x_i, y_i) representing spatial coordinates in a two-dimensional Euclidean space, often characterized by irregular distributions

and high-dimensional variability ("cloud"), we aim to identify and analyze the shape of a void within the cloud.

The identification of voids, cavities, or regions of sparse point density within a point cloud is a pivotal inverse geometry problem with significant implications in computational geometry [1, 2], computer vision [3], computer graphics [4, 5] and robotics [6]. This multifaceted challenge requires an intricate balance between geometric precision and computational practicality [7].

Recently, the importance of void shape analysis in point clouds is increasingly recognized, especially in areas like 3D modeling and reconstruction [8, 9] underlines the growing interest in not just detecting but also understanding the shape and characteristics of voids within point clouds [10].

Traditional methods for void identification in point clouds, primarily density-based techniques [11], focus on calculating point densities to pinpoint potential voids in lower density areas [12]. These methods, including analysis-by-synthesis approaches and nearest neighbor calculations [13], often face challenges with varying density distributions and distinguishing between noise and sparse regions. Graph theory and clustering algorithms like DBSCAN [14] provide insights into point connectivity but may not capture complex spatial relationships inherent in point clouds [15]. Additional geometrical approaches, such as the Ball Pivoting mesh generation algorithm, offer alternative methods for void identification [16, 17], yet they still exhibit limitations in characterizing the intricate details of void structures in refined settings.

To bridge this gap, our approach leverages the mathematical intricacies of Delaunay triangulation [18] alongside the spatial analysis capabilities of Voronoi diagrams [19]. This integration is further enhanced by a new method designed to reconstruct the internal shape of voids using a pseudo-recursive technique. Delaunay triangulation is renowned for its distinctive property, where no point in a set lies within the circumcircle of any triangle in the triangulation. This offers a robust framework for delineating interstitial relationships within a point cloud. Concurrently, the Voronoi diagram, acting as a geometric complement to Delaunay triangulation, counterpart to Delaunay triangulation, provides a natural and intuitive means for assessing point density and spatial interconnections.

Integrating these classical geometric constructs with a robust algorithm inspired by convex hull algorithms [20], our methodology aims to provide a nuanced understanding of voids within point clouds. This approach reconciles the need for geometric accuracy with the inherent variability and complexity of point cloud data, facilitating advanced spatial analysis. We acknowledge the potential computational challenges, such as time complexity and scalability, and aim to address these while balancing precision and practicality.

3 Problem Description: Maximal Internal Envelope (MIE)

Consider a finite set $P = \{p_1, p_2, \dots, p_n\}$, where each $p_i \in \mathbb{R}^2$ represents a point in two-dimensional Euclidean space, denoted as $p_i = (x_i, y_i)$. Our goal is to identify an optimal curve C that accurately delineates the boundary of a low-density region or void within the point cloud. The void is

conceptualized as a region in \mathbb{R}^2 characterized by a low point density.

Given:

- A point cloud P in a two-dimensional space.
- A local density function ρ , derived from Delaunay triangulation and Voronoi diagrams. Delaunay triangulation is used to establish connectivity between points, and the corresponding Voronoi diagram provides insights into the local density and distribution of points. Specifically, larger Voronoi cells indicate lower local densities, which are utilized to define the function ρ .

Objective:

- To identify an optimal curve C that encapsulates the void. The curve should be closed, non-self-intersecting, and optimized to maximize the enclosed area while minimizing its length. The curve's shape, not necessarily convex, reflects the complex nature of void structures in point clouds.

Constraints:

$$C = \underset{C'}{\operatorname{argmin}} \left\{ \operatorname{Length}(C') \left| \begin{array}{l} C' = \bigcup_{i=1}^n [P_i, P_{i+1}], P_{n+1} = P_1, \text{ satisfying:} \\ 1. [P_i, P_{i+1}] \text{ are linear segments, } \forall i \in \{1, \dots, n\} \\ 2. \forall i \neq j, [P_i, P_{i+1}] \cap [P_j, P_{j+1}] = \emptyset \\ 3. \text{ Void is enclosed by } C', \text{ no segments intersect the void} \\ 4. \max \{ \text{Area enclosed by } C' \} \text{ for a given } \operatorname{Length}(C') \end{array} \right. \right\} \quad (1)$$

subject to:

$$C' \text{ maximizes the fidelity to the void's shape,} \quad (2)$$

$$C' \text{ minimizes the deviation from the points defining the boundary of the void,} \quad (3)$$

$$C' \text{ balances the trade-off between simplicity and accuracy.} \quad (4)$$

This problem encapsulates the geometric and computational complexities of identifying and accurately delineating low-density regions within point clouds.

4 Proposed Methodology

The proposed methodology for elucidating the intricate shape characteristics of voids within a two-dimensional point cloud is bifurcated into two distinct stages, each grounded in a combination of geometric and computational strategies.

In the initial stage, our methodology focuses on the broad localization of voids within the point cloud. This stage commences with the identification of principal points delineating the outermost envelope of the cloud, achieved through classical convex hull analysis. The vertices of the convex hull (CH) are then utilized as a basis for defining principal segments across the cloud.

Leveraging Delaunay Triangulation and Voronoi Diagrams in conjunction with the Minimal Distance Scoring (MDS) technique, which we present here, we systematically identify the set of segments that exhibit the highest likelihood of intersecting the void. This technique integrates spatial metrics derived from the triangulation and diagrams to score each segment. We then search for potential first-order Maximal Internal Envelope (MIE) points ($p_i^{MIE} \in P$), based on their proximity and angular relations to these segments.

The second stage adopts an iterative refinement process, building upon the foundational dataset of MIE points from the first stage. Each iteration ("order") enhances the structural definition of the void, iteratively converges towards a nuanced representation of the void's shape.

This 'higher-order' approach, while computationally intensive, allows for a progressively more detailed and accurate delineation of the void's geometry. By iteratively leveraging the MIE points, the methodology converges towards a nuanced and precise representation of the void's fine shape characteristics, thereby encapsulating the complexity and subtlety inherent in the spatial structure of the point cloud.

4.1 Void Identification

The methodology for identifying voids within a two-dimensional point cloud involves a series of geometric and computational steps. We begin by constructing the set of segments connecting all paired Convex Hull vertices, applying the SDS algorithm to assign a Voidness Score parameter to each of the segments to find the segment of maximal likelihood to penetrate the void. We then apply the Delaunay Triangulation and Voronoi Diagrams analysis to identify the optimal point on that segment to represent the point who is considered to be the deepest inside the void. The process involves the following key stages:

4.1.1 Minimal Distance Scoring (MDS)

Definition: The Minimal Distance Scoring (MDS) function evaluates the likelihood of a line segment being within a void. The MDS for a segment L_{ij} connecting points p_i and p_j in P is defined as:

$$\text{MDS}(L_{ij}) = \frac{1}{|P \setminus P_{CH}|} \sum_{p_k \in P \setminus P_{CH}} d(L_{ij}, p_k), \quad (5)$$

where $d(L_{ij}, p_k)$ is the distance from L_{ij} to a point p_k in $P \setminus P_{CH}$.

The principle approach used here for identifying the void is as follows:

- **Convex Hull Identification:** Using an algorithm such as Graham’s Scan or Jarvis’s March [20], the Convex Hull P^{CH} of P is identified.
- **Starting Point Selection:** A point P_i^{CH} is selected from the subset P^{CH} . This selection can be randomized within P^{CH} or based on a geometric heuristic, such as the point’s centrality or distance to other points in P^{CH} .
- **Segment Creation and Analysis:** For each P_i^{CH} , segments L_{ij} connecting it to other points in P^{CH} are created. These segments are analyzed for their potential to intersect the internal void.
- **Voidness Score Calculation:** The voidness score $V(L_{ij}) = \text{MDS}(L_{ij})$ (see Equation 5) for each segment L_{ij} is calculated as the average distance to points in $P \setminus P^{CH}$. The segment with the lowest voidness score is selected as L_{ij}^{best} and is considered to have a greater potential to be close to or within the internal void.

4.1.2 Delaunay-Voronoi (DV) point selection

Using Delaunay Triangulation and Voronoi Diagrams, we select the optimal point on L_{ij}^{best} that best represents the area with the lowest density in the point cloud.

Delaunay Triangulation: Given a set of points P in a two-dimensional Euclidean space, a Delaunay triangulation for P is a triangulation $\text{DT}(P)$ such that no point in P is inside the circum-circle of any triangle in $\text{DT}(P)$.

Properties:

- Maximizes the minimum angle of all the angles of the triangles in the triangulation, avoiding narrow triangles.
- The triangulation is unique if no four points are cocircular.
- Each triangle’s circumcircle contains no other points from P in its interior.

Voronoi Diagrams: The Voronoi diagram for a set of points P in a two-dimensional space partitions the plane into regions where each region corresponds to a point in P . For each point $p_i \in P$, its corresponding Voronoi cell, denoted as $V(p_i)$, consists of all points closer to p_i than to any other point in P .

Properties:

- Each Voronoi cell $V(p_i)$ is a convex polygon.
- The diagram is the dual graph to the Delaunay triangulation of P .

- The edges of the Voronoi diagram are perpendicular bisectors of the edges of the Delaunay triangulation.

The point that best represent the area with lowest density of cloud point is selected as the DV point.

4.1.3 Schematic Algorithm

The process is schematically represented below 1, detailing the computational steps for void identification.

Table 1: Algorithm for Void Identification

Step	Action
1:	Identify Convex Hull P^{CH} of P
2:	Select a starting point P_i^{CH} from P^{CH}
3:	For each P_i^{CH} , create and analyze segments L_{ij}
4:	Calculate $MDS(L_{ij})$ for each segment
5:	Select L_{ij}^{best} with minimum MDS value
6:	Apply Delaunay Triangulation and Voronoi Diagrams to select DV point on L_{ij}^{best}

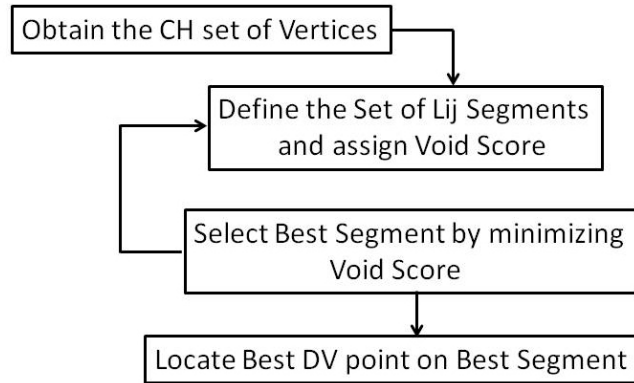


Figure 1: Schematic Algorithm for Void Identification.

4.2 Void Shape Construction

The final stage involves constructing the shape of the void using an expanding polygon methodology, initiated from the segment L_{ij}^{best} identified by the MDS algorithm. This approach combines

computational geometry techniques with iterative algorithms to accurately model the void's shape. A schematic representation of the above is shown for clarity below 2.

4.2.1 Polygon Construction

- **Vertex Selection:** The vertices of the expanding polygon, denoted by the set $C \subseteq P$, are chosen based on their proximity to L_{ij}^{best} . The process begins with a minimal set of points in C and expands by adding new vertices from P .
- **Initial Configuration:** The process initiates with an imaginary circle centered at the DV point on the segment L_{ij}^{best} . This circle gradually expands in radius until it first intersects with points in the cloud. The center of the circle then traverses along the segment L_{ij}^{best} , extending towards both endpoints in predefined step sizes (controlled by parameter $3 \leq k \leq n$). Throughout this traversal, points that are first intersecting with the expanding circle are accumulated into the set C , forming the initial vertex set for the polygon. This procedure is systematically repeated for all segments L_{ij} associated with P_i^{CH} , ensuring comprehensive coverage and inclusion of relevant points in the vicinity of the void.
- **Growth Algorithm:** Starting with the initial set of Maximal Internal Envelope (MIE) points in C , the algorithm enters an iterative phase, where each iteration is marked by an increasing "Order" of complexity and refinement. At each iteration, the algorithm constructs all possible segments connecting the vertices currently in C . For each of these segments, the imaginary circle process is reapplied. This process involves centering an imaginary circle on various points along each segment and expanding it until it first intersects with a new point in the cloud. The newly intersected point, not previously included in C , is then added to the MIE collection. This iterative expansion and addition of points to C continues, thereby progressively refining and elaborating the polygonal representation of the void's boundary with each successive order.
- **Constraint by Points in P :** As the polygon expands, its growth is influenced by the fixed points in P . These points act as constraints, guiding the polygon's expansion. When a potential expansion intersects with a point in P , that point becomes a candidate to be added as a new vertex to the polygon. This process ensures that the expanding polygon adapts its shape to encompass the void, respecting the spatial distribution of P .
- **Intersection Condition:**
 - A point $p \in P$ is considered to intersect with the expanding polygon if the distance from p to the nearest line segment of the polygon is less than a predefined constant δ .
 - Points satisfying this condition are incorporated into the set C , altering the polygon's shape.
- **Adaptive Shape Modification:** The shape of the polygon at each stage of expansion is a collection of line segments connecting adjacent vertices in C . This means the polygon is always a closed, piecewise-linear path. The algorithm ensures that with each expansion

step, the polygon remains a valid geometric shape. It dynamically adjusts the polygon by adding new vertices, removing redundant ones, or altering the connections between vertices to best represent the boundary of the void.

- **No Internal Points Assumption:** It is assumed that no point in P reside insides the expanding polygon. Under this assumption, a void cannot be defined as such if it contains points within.
- **Computational Implementation:** Implementing these dynamics requires an iterative process where the polygon’s shape is continuously updated. Each iteration involves checking for potential expansions, evaluating constraints from P , and updating C and the polygon’s edges accordingly. Data structures, such as priority queues [21], might be used to efficiently manage potential expansion candidates based on their geometrical locations relative to cloud points $p_i \in P$.

Through these dynamics, the expanding polygon evolves in a manner that is both controlled by an internal growth logic and responsive to the external environment defined by the points in P . This dual influence ensures that the polygon effectively and accurately delineates the shape of the void.

4.2.2 Refining Criterion

- Define a ‘Refining’ parameter $k = 1/\delta$ of the expanding polygon, representing the number of steps along L_{ij}^{best} . This parameter is employed by the algorithm to facilitate the pursuit of an additional intersecting point, thereby enhancing the refinement process.
- The refining ranges from a minimum of 3 with a practical upper limit of n , the number of points in P .
- The expansion process is observed through increasing orders, providing a measure for the growth and adaptation of the expanding polygon to the void’s shape.

Table 2: Algorithm for Void Shape Construction

Step	Action
1:	Identify segments L_{ij}^{best} with minimum MDS value.
2:	Along each segment L_{ij}^{best} , define a dynamic imaginary circle that expands from the DV point.
3:	Identify Maximal Internal Envelope (MIE) points from P that intersect with the expanding circle.
4:	Incorporate these intersecting points into the subset C .
5:	Update the set C and repeat the process for the new segments formed.
6:	Terminate the iterative process when the addition of new points to C ceases.

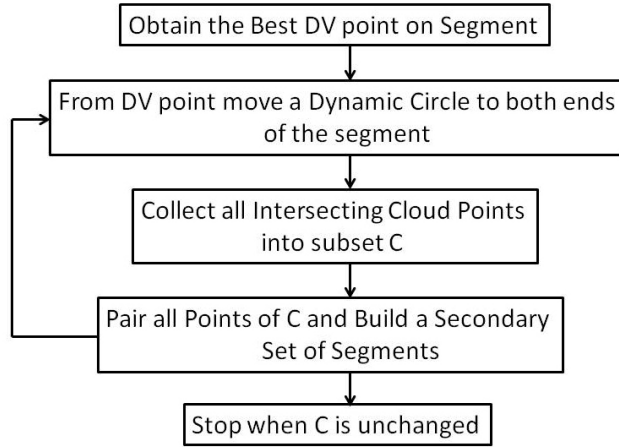


Figure 2: Schematic Algorithm for Void Shape Construction.

4.3 Complexity Analysis

Given a 2D point cloud with n points, we aim to analyze the complexity of the process as described above for void identification and shape construction:

1. Compute the convex hull of the point cloud.
2. Generate all unique pairs of vertices on the convex hull.
3. Generate pairs from a subset of points (approximately 1/10th the size of the original set) and repeat this step up to a maximal order of 3.

Detailed Considerations

- **Convex Hull Calculation:** The convex hull of a point cloud is computed, which typically has a complexity of $O(n \log n)$.
- **Pair Generation of Convex Hull Vertices:** Assuming the convex hull has approximately $\frac{n}{10}$ vertices, the number of pairs generated is $\binom{\frac{n}{10}}{2} \approx \frac{n^2}{200}$. Hence, the complexity for this step is $O\left(\frac{n^2}{100}\right)$.
- **Subset Pair Generation:** For a subset of points similar in size to the convex hull vertices, the complexity for pair generation remains $O\left(\frac{n^2}{100}\right)$. However, for moderate-sized n , this quadratic term is manageable and does not drastically impact performance.
- **Repetitions:** Repeating the pair generation for subsets twice more adds a cumulative complexity of $2 \times O\left(\frac{n^2}{100}\right)$.

Overall Complexity Combining all steps, the total complexity is:

$$O(n \log n) + 4 \times O\left(\frac{n^2}{100}\right) \quad (6)$$

This expression shows that while the convex hull computation is $O(n \log n)$, the pair generation steps, particularly for larger n , contribute a significant quadratic component to the overall complexity. Given the moderate size of n , this complexity is generally well-handled by contemporary computational resources.

The study underscores the need for optimizing such algorithms, particularly for applications dealing with extensive spatial datasets. In scenarios involving moderate-sized 2D point clouds however, the complexity of the algorithms used for convex hull computation and pair generation, does not pose significant challenges. This above analysis demonstrates that such tasks are computationally feasible within the constraints of typical processing capabilities.

5 Results - Void Identification and Shape Construction

In the present study, two distinct ensembles of 2D point sets were employed to illustrate the construction of the Maximal Internal Envelope (MIE) shape: a canonical circle with random distribution along the circumference, and a pair of congruent circles offset by half a radius with an internal void. The Convex Hull vertices for each case were computed, as shown in Figure 3.

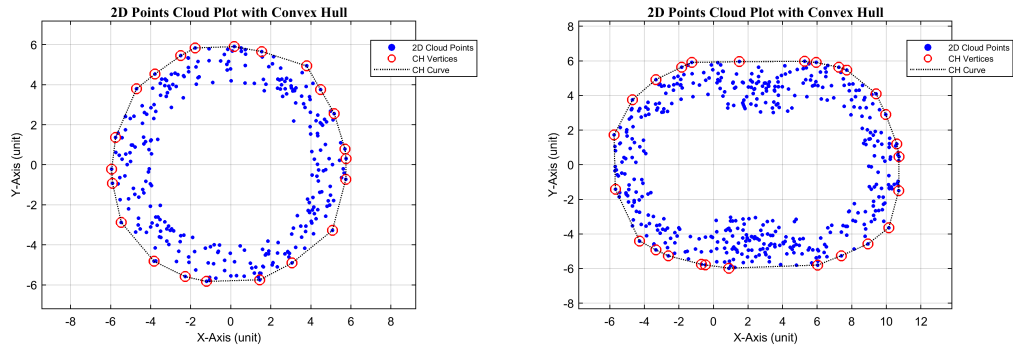


Figure 3: The 2D point distributions of a shell-like circle (left) and a moderately detailed shape (right).

We initiated by selecting optimal segments from the Convex Hull points, aiming to identify those traversing the void. Delaunay triangulation and Voronoi diagrams were then used to determine the starting point for the envelope construction (see in Figure 4). The process involved projecting an imaginary circle from the Delaunay-Voronoi (DV) point along the selected segment. Points intersecting with this circle, as shown in Figure 5, were included in the subset $C \subseteq P$.

These points, representing the Maximal Internal Envelope (MIE), were instrumental in outlining the curve that encapsulates the internal void, thereby providing a detailed and quantifiable representation of its spatial characteristics.

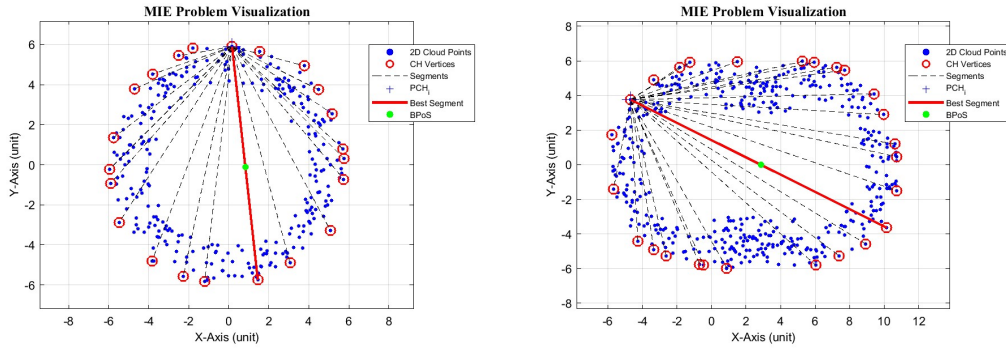


Figure 4: Example of best segments selection based on MDS for the two clouds. Every segment is connecting CH pairs of the respective 2D points distribution.

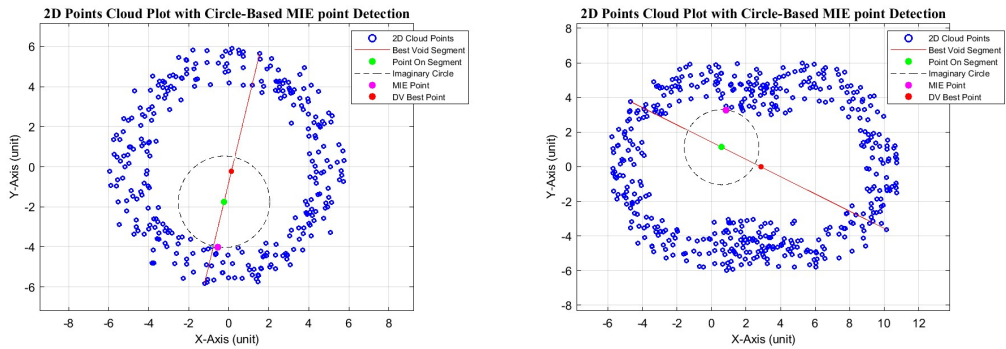


Figure 5: Example of MIE points identification based on best segment and VD starting point on segment for the interior void polygon construction.

The resultant shapes of the Maximum Internal Envelope (MIE) for the two aforementioned scenarios are presented in a comparative analysis, catering to distinct settings of the parameter k and increasing orders of calculations. Specifically, we exhibit the MIE configurations for $k = 3$ and $k = 31$,¹ and different calculation orders. Table 3 shows the convergence orders for the cases simulated here. The respective visual representations of these MIE shapes are illustrated in Figures 6 for the circle-shaped cloud, and 7 for the dual-circles-shaped cloud with $k = 3$.

¹These values were selected arbitrarily to showcase the approach's versatility and scalability under various conditions.

Table 3: Data Summary

Shape	k-value	Orders
1 Circle	3	23
1 Circle	31	18
2 Circles	3	31
2 Circles	31	22

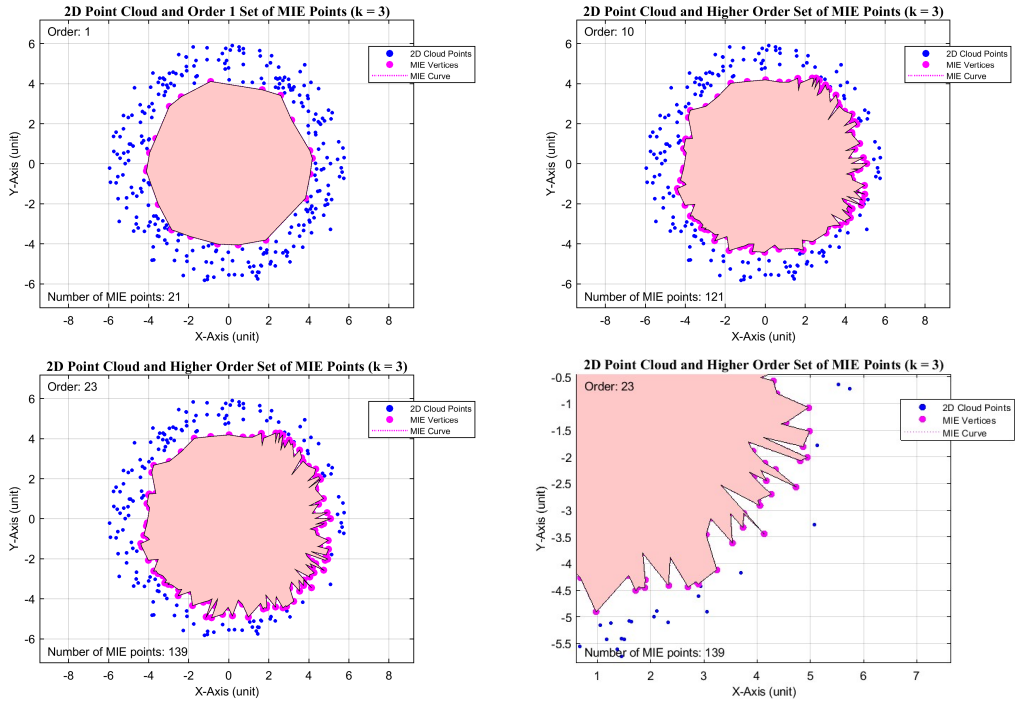


Figure 6: The final maximal interior void in the single-circle shape with different orders for $k = 3$.

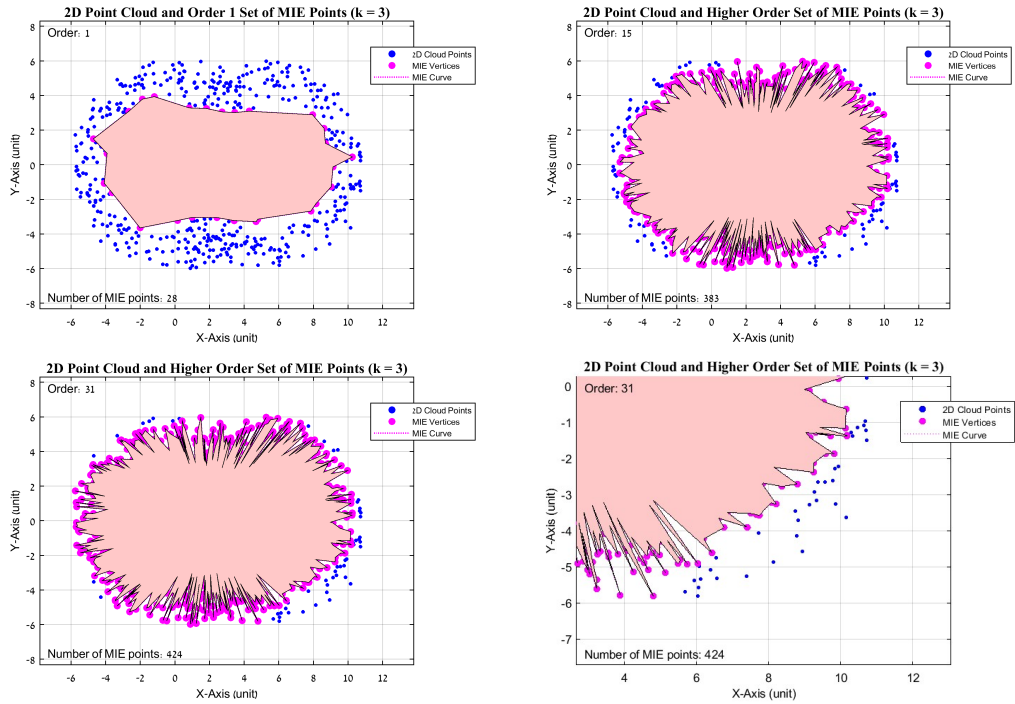


Figure 7: The final maximal interior void in the dual-circles shape with different orders for $k = 3$.

The figures in 8 display the number of MIE points identified at various orders for $k = 3$ and $k = 31$ in both the single-circle and dual-circle scenarios. These values are derived from the full spectrum of orders (iterations) conducted during our simulations.

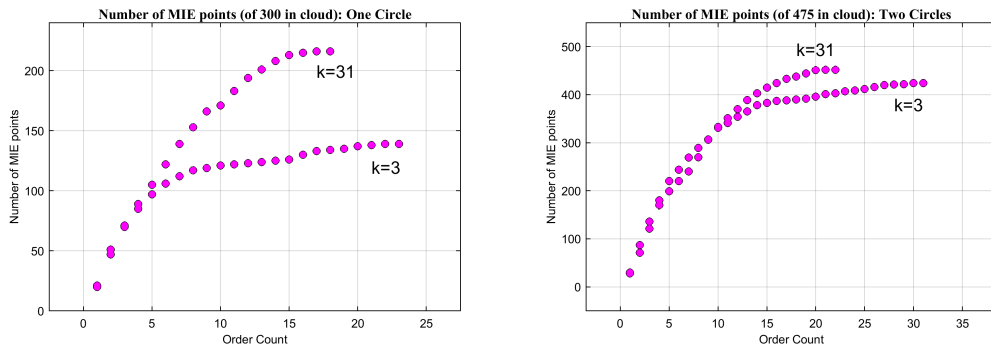


Figure 8: Number of MIE points as a function of the calculation order for the dual-circles shape.

In the course of our study, several key observations emerged that merit detailed consideration:

- **Precision in Internal Void Identification:** The methodology employed in our study has demonstrated high accuracy in the delineation of internal voids. These voids were not only clearly identified but also faithfully represented in terms of their visual and geometric properties. This fidelity is crucial, as it underscores the reliability of our approach in capturing the intrinsic features of voids within different geometrical structures.
- **Efficacy of Convex Hull Points in Segment Definition:** The utilization of convex hull points as the basis for defining segments has proven to be effective. Nonetheless, it is pertinent to acknowledge that exploring a broader spectrum of segment definition methodologies could potentially enhance the granularity and intricacy of the void structure revelation. This exploration could lead to a more nuanced understanding of the internal geometry of complex shapes.
- **Impact of Parameter k on Void Structure Refinement:** Our findings clearly indicate that increasing the value of k substantially improves the refinement of the internal void structure. This enhancement is attributed to the increased number of steps taken along the segment with the highest probability of being situated within the void. The correlation between k and the detail in void representation is pivotal, as it demonstrates the tunability and adaptability of our approach to different granularity levels.
- **Fine Coverage in High Order Calculations:** As expected, higher orders result in the identification of more MIE points. Importantly, these points consistently provide valid coverage of the void's area in all cases, ensuring continuous spatial representation. The determination of the void's true shape, however, is semantic and highly dependent on both the setting of k and the degree of the calculation order.

6 Conclusions

This study introduces a method for identifying and characterizing voids within two-dimensional point clouds, leveraging the synergistic integration of Delaunay triangulation, Voronoi diagrams, and Minimal Distance Scoring. The study highlights the method's efficacy in accurately delineating internal voids and its adaptability to diverse geometric configurations.

6.1 Key Findings and Methodological Developments

- The proposed method has demonstrated high accuracy in delineating internal voids, capturing their intrinsic geometric properties with high fidelity.
- The effectiveness of using convex hull points for segment definition was affirmed, with the potential for further enhancement through exploration of alternative segment definition methodologies.
- A significant correlation was observed between the parameter k and the level of detail in void representation, illustrating the method's adaptability in refining the internal void structure.

- The method exhibited robustness in reconstructing void shapes across different point cloud configurations, from simple symmetric circles to more complex structures.

6.2 Limitations and Future Directions

- The current study did not prioritize computational efficiency, presenting an avenue for future optimization, especially for handling large-scale datasets.
- The method's efficacy in dealing with highly detailed voids remains to be tested and will form a critical part of our ongoing research.
- Future work may also explore the integration of machine learning techniques to further refine the void identification process and automate certain aspects of the methodology.
- The principles and algorithms utilized in this study suggest potential for generalization to higher-dimensional spaces. This aspect may enable broader applicability in analyzing more complex spatial data, warranting further investigation.
- The computational complexity analysis reveals that while the convex hull computation is efficient, the quadratic nature of pair generation steps, especially for larger datasets, necessitates optimization for applications with extensive spatial data.

In conclusion, acknowledging the need for further research, this study concentrates on the broader field of geometric data interpretation and may offer a basis for future developments in various domains of spatial data processing for voids identification within spatial points distributions.

Declarations

All data-related information and coding scripts discussed in the results section are available from the corresponding author upon request.

References

- [1] P. Bubenik. Statistical Topology Using Persistence Landscapes. *SAO/NASA Astrophysics Data System*, 2012.
- [2] P. Chalmoviansky and B. Juttler. Filling Holes in Point Clouds. In *Filling Holes in Point Clouds*, pages 196-212. 2003. ISBN 978-3-540-20053-6. DOI: 10.1007/978-3-540-39422-8_14.
- [3] H. Jiang, Y. Lu, and S. Chen. Research on 3D Point Cloud Object Detection Algorithm for Autonomous Driving. *Mathematical Problems in Engineering*, 2022, pages 13. DOI: 10.1155/2022/8151805.

- [4] K. Salvaggio and C. Salvaggio. Automated identification of voids in three-dimensional point clouds. *Proc SPIE*, 8866, 2013. DOI: 10.1117/12.2023740.
- [5] J. Deng, S. Shi, P. Li, W. Zhou, Y. Zhang, and H. Li. Voxel R-CNN: Towards High Performance Voxel-Based 3D Object Detection. In *AAAI Conference on Artificial Intelligence*, pages 1, 2, 6, 7, 8, 2021.
- [6] K. Abdel-Malek, H.-J. Yeh, and S. Othman. Interior and exterior boundaries to the workspace of mechanical manipulators. *Robotics and Computer-Integrated Manufacturing*, 16(5):365-376, 2000. DOI: [https://doi.org/10.1016/S0736-5845\(00\)00011-9](https://doi.org/10.1016/S0736-5845(00)00011-9).
- [7] K. N. Salvaggio, C. Salvaggio, and S. Hagstrom. A voxel-based approach for imaging voids in three-dimensional point clouds. In *Geospatial InfoFusion and Video Analytics IV; and Motion Imagery for ISR and Situational Awareness II*, SPIE, 9089, pages 90890E, 2014. DOI: 10.1117/12.2050425.
- [8] B. Fei, W. Yang, W.-M. Chen, Z. Li, Y. Li, T. Ma, X. Hu, and L. Ma. Comprehensive Review of Deep Learning-Based 3D Point Cloud Completion Processing and Analysis. *IEEE Transactions on Intelligent Transportation Systems*, 23(12):22862-22883, 2022. DOI: 10.1109/TITS.2022.3195555.
- [9] C.-H. Huang and C.-C. Shih. A shape identification problem in estimating simultaneously two interfacial configurations in a multiple region domain. *Applied Thermal Engineering*, 26(1):77-88, 2006. DOI: <https://doi.org/10.1016/j.applthermaleng.2005.04.019>.
- [10] F. Hoyle and M. S. Vogeley. Voids in the Point Source Catalogue Survey and the Updated Zwicky Catalog. *The Astrophysical Journal*, 566(2):641, 2002. DOI: 10.1086/338340.
- [11] Q. Hu and Y.-J. Shen. CA mortar void identification for slab track utilizing time-domain Markov chain Monte Carlo-based Bayesian approach. *Structural Health Monitoring*, 22(6):3971–3984, 2023. DOI: 10.1177/14759217231166117.
- [12] A. Srivastava and I. H. Jermyn. Looking for Shapes in Two-Dimensional Cluttered Point Clouds. *IEEE Transactions on Pattern Analysis and Machine Intelligence*, 31(9):1616-1629, 2009. DOI: 10.1109/TPAMI.2008.223.
- [13] V. Nguyen, T. Trinh, and M. Tran. Hole Boundary Detection of a Surface of 3D Point Clouds. In *2015 International Conference on Advanced Computing and Applications (ACOMP)*, pages 124-129, 2015. DOI: 10.1109/ACOMP.2015.12.
- [14] E. Schubert, J. Sander, M. Ester, H. P. Kriegel, and X. Xu. DBSCAN Revisited, Revisited: Why and How You Should (Still) Use DBSCAN. *ACM Trans. Database Syst.*, 42(3), 2017. DOI: 10.1145/3068335.
- [15] K. Abdel-Malek, H.-J. Yeh, and S. Othman. Swept volumes: void and boundary identification. *Computer-Aided Design*, 30(13):1009-1018, 1998. DOI: [https://doi.org/10.1016/S0010-4485\(98\)00054-2](https://doi.org/10.1016/S0010-4485(98)00054-2).

- [16] Thomas Wright and Barry Lennox. Algorithmic Approach to Planar Void Detection and Validation in Point Clouds. In *Towards Autonomous Robotic Systems*, Springer International Publishing, pages 526–539, 2017. ISBN: 978-3-319-64107-2.
- [17] B. Bird, B. Lennox, S. Watson, and T. Wright. Autonomous Void Detection and Characterisation in Point Clouds and Triangular Meshes. *International Journal of Computational Vision and Robotics*, 9(4):368-386, 2019. DOI: 10.1504/IJCVR.2019.101538.
- [18] D. J. Mavriplis. An Advancing Front Delaunay Triangulation Algorithm Designed for Robustness. *Journal of Computational Physics*, 117(1):90-101, 1995. DOI: <https://doi.org/10.1006/jcph.1995.1047>.
- [19] A. Okabe, T. Satoh, T. Furuta, A. Suzuki, and K. Okano. Generalized network Voronoi diagrams: Concepts, computational methods, and applications. *International Journal of Geographical Information Science*, 22(9):965-994, 2008. DOI: 10.1080/13658810701587891.
- [20] F. P. Preparata and S.J. Hong. Convex Hulls of Finite Sets of Points in Two and Three Dimensions. *Commun. ACM*, 20(2):87–93, 1977. Publisher: ACM.
- [21] R. Kumar. *Book Chapter - QUEUEING SYSTEM*. Springer, 2020, pp. 1-31. ISBN 9789385935732.